NANO LETTERS

Letter

pubs.acs.org/NanoLett

Imaging Nanometer Phase Coexistence at Defects During the Insulator–Metal Phase Transformation in VO_2 Thin Films by Resonant Soft X-ray Holography

Luciana Vidas,[*,†] Christian M. Günther,[‡] Timothy A. Miller,[†] Bastian Pfau,[§] Daniel Perez-Salinas,[†] Elías Martínez,[†] Michael Schneider,[§] Erik Guehers,[‡] Pierluigi Gargiani,[∥] Manuel Valvidares,[∥] Robert E. Marvel,[⊥] Kent A. Hallman,[⊥] Richard F. Haglund, Jr.,[⊥] Stefan Eisebitt,[‡,§] and Simon Wall[*,†]

[†]ICFO—Institut de Ciències Fotòniques, The Barcelona Institute of Science and Technology, Castelldefels, 08860 Barcelona, Spain

[‡]Institut für Optik und Atomare Physik, Technische Universität Berlin, 10623 Berlin, Germany

[§]Max-Born-Institut, 12489 Berlin, Germany

[∥]ALBA Synchrotron Light Source, Cerdanyola del Vallès, E-08290 Barcelona, Spain

[⊥]Department of Physics and Astronomy, Vanderbilt University, Nashville, Tennessee 37235-1807, United States

S *Supporting Information*

ABSTRACT: We use resonant soft X-ray holography to image the insulator–metal phase transition in vanadium dioxide with element and polarization specificity and nanometer spatial resolution. We observe that nanoscale inhomogeneity in the film results in spatial-dependent transition pathways between the insulating and metallic states. Additional nanoscale phases form in the vicinity of defects which are not apparent in the initial or final states of the system, which would be missed in area-integrated X-ray absorption measurements. These intermediate phases are vital to understand the phase transition in VO_2, and our results demonstrate how resonant imaging can be used to understand the electronic properties of phase-separated correlated materials obtained by X-ray absorption.

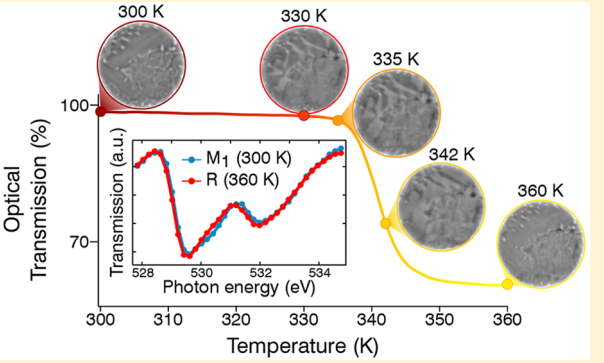

KEYWORDS: *VO_2, phase transition, imaging, resonant holography, phase separation, XAS*

Electronic correlations and structural distortions play a strong role in the physics of the system of VO_2, a prototypical correlated material. At approximately 65 °C, VO_2 undergoes a first order phase transformation from monoclinic (M_1) insulating phase to rutile (R) metallic phase.[1] The mechanism responsible for the phase transition has been difficult to determine, and it is an open question whether the structural distortion alone can account for the opening of the band gap, or if electronic correlations are additionally required. Theoretical evidence for strong electronic correlations is mixed. Density functional theory (DFT) in the local density approximation predicts that the M_1 state should be metallic, which suggests that correlation effects, which are not included in DFT, may be responsible for the band gap. However, recent DFT calculations with more sophisticated functionals[2] can reproduce a gaped state for the M_1 phase without correlations, but other issues are known to occur.[3] As a result the role played by correlations is still open.

Experimentally it is hard to separate the contributions of electronic correlations from the structural change. In some thin films the metallicity is believed to precede the structural change,[4−7] and nanoscale infrared imaging has also shown that there are unusual transport properties near T_c.[8] Observation of a monoclinic metal could indicate that correlations play a key role in determining the metallic properties of the material as the strength of the correlations can change the size of the band gap without a change in lattice symmetry. Recently, Gray et al.[9] argued that soft X-ray absorption spectroscopy (XAS) can be used to measure the strength of electronic correlations separate from the structural phase transition and from the temperature dependence of the XAS signal suggested that the correlations weaken before the structural changes occur. However, no technique to date has been able to directly probe both structural and electronic aspects simultaneously while maintaining sufficient spatial resolution to ensure homogeneous probing. This is an issue because, while high-quality single crystals show that structural and electronic changes are concomitant and occur within 0.01 K,[10] the thin films that show monoclinic metallic phases have transitions regions which are several degrees wide in temperature. This demonstrates that

Received: February 1, 2018
Revised: May 11, 2018
Published: May 16, 2018

DOI: 10.1021/acs.nanolett.8b00458
Nano Lett. XXXX, XXX, XXX−XXX

the phase transition in thin films is heterogeneous, and phase coexistence occurs during the transition. This is a particular concern in VO_2, as it is known that, in ambient conditions, it is close to a solid-state triple point with a second monoclinic insulating state (M_2).[1] Due to the first order nature of the phase transition, these phases may also coexist,[11−13] which makes separating out the roles of each phase more of a challenge.

To address this point, we build on the work by Gray et al.[9] and use polarization and wavelength resolved X-ray holography to image both the structural and the electronic correlation aspects of the insulator-to-metal phase transition in thin films of VO_2 with the same technique and with 50 nm spatial resolution. We observe that, depending on the local environment, the sample can take two pathways. One is the direct transition, in which the material transforms directly between the M_1 and R phases. The other path is an indirect transition through an intermediate phase. While this phase could be ascribed to the monoclinic metallic state, we believe it is more likely to be the insulating M_2 phase. The distinct pathways result from nanoscale defects that modulate the strain environment locally within the sample. Our results highlight the key role played by defects in the phase transition in VO_2 and the power of resonant holography for studying phase separation in correlated materials on the nanoscale.

Resonant soft X-ray holography is a lensless imaging technique that can exploit the full power of element and polarization specificity of X-ray absorption spectroscopy for contrast in imaging.[14] As holography is an interference-based imaging technique, it is sensitive to the relative shifts of the amplitude and phase of the transmitted light across the sample. Thus, it is particularly suited for measuring phase-separated materials, which modulate the local transmission. A schematic band diagram for the states probed by XAS on VO_2 is shown in Figure 1a, based on the Goodenough model,[15] for the M_1 and R phases. In this simplified picture, which does not include correlations, the π levels are bonding/antibonding states that result from a hybridization of the vanadium 3d and oxygen 2p orbitals, whereas the $d_{\|}$ states result from the overlap between vanadium ions along the rutile *c*-axis. The monoclinic distortion splits the $d_{\|}$ band and moves the π^* orbital above the Fermi level.

This simple model can qualitatively explain most of the XAS features. Spatially integrated XAS measurements on our VO_2 thin films on free-standing Si_3N_4 membranes are shown in Figure 1b (see the Supporting Information for sample details). Due to the strong hybridization between the oxygen 2p and vanadium 3d levels, XAS spectra at the oxygen K-edge also probe the 3d orbitals of the vanadium ions. In the Goodenough picture, the bottom of the conduction band is the π^* band, which is derived from the isotropic V d_{xy} and d_{yz} orbitals. In the R state, the π^* band moves below the Fermi level, resulting in an increase in absorption at lower energies, as observed. The $d_{\|}$ bands are derived from the V $d_{x^2-y^2}$ orbitals, which are strongly anisotropic. Transitions into the $d_{\|}$ states are only observed when the electric field vector is parallel to the rutile *c*-axis. When the $d_{\|}$ band is split due to the structural distortion in the low-temperature phase, an additional higher-energy absorption process is observed as indicated in Figure 1b. This polarization-sensitive $d_{\|}$ peak allows measurement of both the structural transition and the orientation of the sample *c*-axis.

Although the Goodenough model predicts an isotropic π^* conduction band, the XAS shows a small, polarization-dependent shift[16] indicated as $d_{\|}^c$ in the inset of Figure 1b in

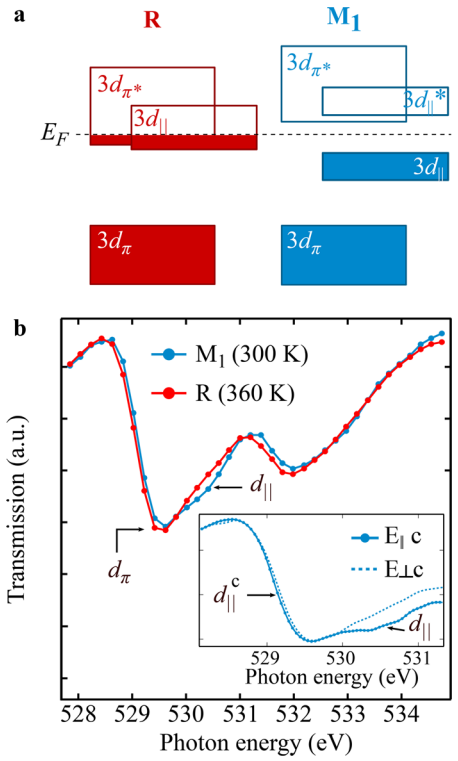

Figure 1. Electronic structure and X-ray transmission of VO_2. (a) Schematic of the band structure proposed by Goodenough.[15] The π states are hybridized vanadium 3d and oxygen 2p orbitals. The $d_{\|}$ state forms from overlapping vanadium d orbitals along the rutile *c*-axis. (b) X-ray absorption spectra of the oxygen edge showing the transition to the π^* and $d_{\|}$ states measured in transmission. The inset shows normalized spectra at room temperature, in the M_1 phase, for X-rays parallel and perpendicular to the rutile *c*-axis. The polarization-dependent edge shift, labeled $d_{\|}^c$, corresponds to the contribution from the $d_{\|}$ state due to the formation of correlated dimers.[16,17]

the monoclinic phase. This feature is often ascribed to effects resulting from electronic correlations,[9,16] as it is found in cluster dynamical mean field theory calculations,[17] where electronic correlations were shown to provide an additional contribution from the $d_{\|}$ states to the bottom of the conduction band due to the formation of a correlated vanadium singlet state in the monoclinic phase. This feature is lost when the singlets are broken in the metallic phase and can thus be used to measure correlations in the insulating phase of VO_2.

Based on the temperature dependence of the XAS dichroism of the $d_{\|}$ and $d_{\|}^c$ states, Gray et al.[9] argued that the singlet state is lost 7 K below the temperature at which the conventional structural phase transition occurs, and interpreted this as a sign of weakening electronic correlations prior to the structural transition. This may explain the origins for monoclinic-like metallic phases that have been observed,[4−6] which also occur near the conventional structural transition temperature. However, in this temperature range, both the metallic and insulating phases have been observed to coexist, and from area-integrated XAS measurements, it is not clear if the loss of correlations is homogeneous or heterogeneous across the sample, or if nanoscale phase coexistence may affect the interpretation of the spectra. With resonant soft X-ray holographic imaging we can directly address this issue.

Figure 2a shows a scanning electron microscopy (SEM) image of a VO_2 sample. Samples were fabricated through pulsed

DOI: 10.1021/acs.nanolett.8b00458
Nano Lett. XXXX, XXX, XXX−XXX

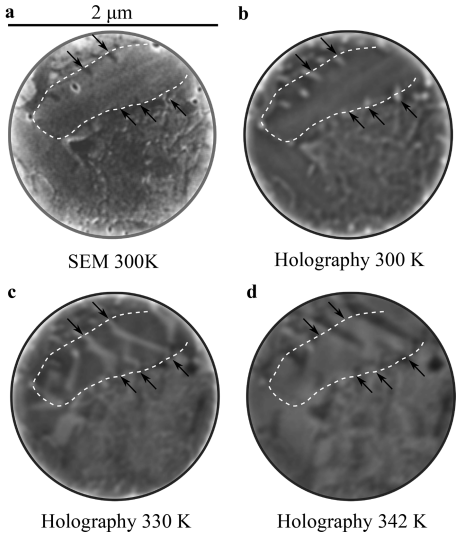

Figure 2. (a) SEM images of the VO_2 sample show that large single crystals grow together with nanoscale crystallites. The dotted white line indicates the perimeter of a single crystal. On the edges of the crystal, several defects are observed (some indicated with arrows). (b) Holographic image of the same sample imaged at 530.5 eV at room temperature, showing good agreement with the SEM image. (c) Same sample heated to 330 K, i.e., close to the transition temperature ($T_c \approx$ 340 K). Thin stripes appear spanning the single crystal corresponding to the metallic phase. (d) At a higher temperature, after T_c, the metallic domains grow bigger until the whole sample becomes metallic.

laser deposition on Si_3N_4 membranes and were shown to be in the M_1 phase with Raman scattering (further details can be found in the Supporting Information). Although our substrate is amorphous, we occasionally find regions of the sample with micron-sized single crystals among smaller crystallites, and we focus on those in our study as indicated in Figure 2. On the perimeter of these single crystals, several defects can be observed, with features as small as 50 nm. In Figure 2b, we image the same sample via X-ray holography with X-rays tuned to the $d_{\|}$ peak, which provides maximum contrast for the insulator−metal transition. At room temperature, we see excellent agreement between the SEM and holographic images given the different contrast mechanism of both techniques, demonstrating the adequate spatial resolution of our method. When we heat the sample to 330 K, i.e., to the start of the phase transition in our films, we see bright stripes appearing across the crystallite (Figure 2c). These stripes are metallic filaments that are observed because the sample has a higher transmissivity when metallic at the photon energy corresponding to the $d_{\|}$ XAS feature. Interestingly, these domains, while long, can be as narrow as 50 nm. It is clear from the evolution with temperature that the nanoscale defects nucleate the metallic phase and form metallic domains that span between defects, demonstrating the role of local strain in locally lowering the transition temperature. A further increase in temperature results in the growth of these filaments (Figure 2d) until the whole sample becomes metallic. As these defects appear dark in the SEM and bright in holography, indicating high transmission, we associate these defects with grain boundaries between VO_2 crystallites. In fact, nucleation points at VO_2 grain boundaries are consistent with previous work which showed how oxygen vacancies created by strain at grain boundaries present a decreased phase-transition energy.[18]

We now turn to investigate the role of electronic correlations and the presence of other phases in the growth of the metallic phase at the insulator−metal transition. To do this, we perform spectrally resolved imaging at multiple X-ray wavelengths. This imaging is performed in a different sample to that shown in Figure 2, with the X-rays polarized along the rutile *c*-axis, as made evident in the X-ray dichroic contrast shown in Figure S4 in the Supporting Information. We collect X-ray holograms at 518 eV incident photon energy on the vanadium L_2-edge, which is also sensitive to the $d_{\|}$ states,[19] at 529 eV to be sensitive to the π^* and $d_{\|}^c$ levels, and at 530.5 eV to be resonant to transitions into the $d_{\|}$ states. We then use the images obtained at these three photon energies to encode the red (518 eV), blue (529 eV), and green (530.5 eV) channels of a false-color image. In this spectral fingerprinting approach, we can observe if changes occur in different regions of the sample and at different temperatures. For example, if electronic correlations precede the structural transition as observed by Gray et al.,[9] then the $d_{\|}^c$ (blue channel) will change before the $d_{\|}$ (green channel), resulting in a change of color in the image.

Figure 3 shows the spectrally resolved changes as a function of temperature. Again, we see the formation of nanoscale

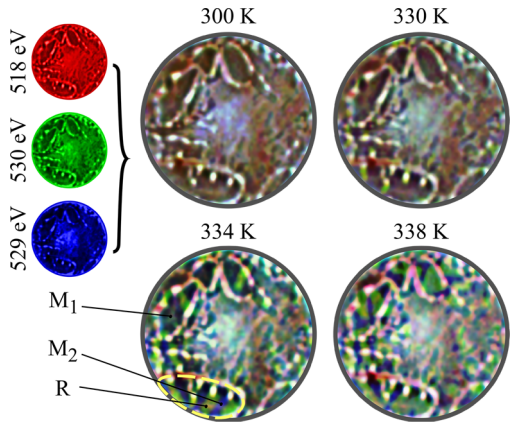

Figure 3. Spectrally resolved images at the vanadium and oxygen edges. The images are recorded at 518, 529, and 530.5 eV and are used to encode the intensities of the three color channels of an RGB (red, green, blue) image. At 330 K, an increase in intensity of the green channel, which probes the rutile phase through the $d_{\|}$ state, is observed in small regions similar to that observed in Figure 2. As the sample is heated further, it becomes increasingly clear that the blue channel, which probes the $d_{\|}^c/d_{\pi}^*$ state, also changes but in different regions. At 334 K, three distinct regions can be observed corresponding to the monoclinic M_1, M_2, and R phases. As the temperature increases, the R phase dominates. The dashed line corresponds to the ROI shown in Figure 4. The circular field of view is 2 μm in diameter.

domains that span the small single crystals, starting at defects. However, now we can see that in different regions of the sample the X-ray transmission changes differently. At 334 K, we can discern at least three different phases as indicated: the original M_1 phase and two new phases, one with a subtle change in the $d_{\|}^c$ (blue) channel and a second one with the greater change in the $d_{\|}$ (green) channel.

To understand how these phases grow, we perform a finer temperature scan and focus on one of the small single crystals indicated in Figure 3. In addition, to amplify the changes we threshold each channel (see the Supporting Information) and show images at key temperatures in Figure 4a. At low

DOI: 10.1021/acs.nanolett.8b00458
Nano Lett. XXXX, XXX, XXX−XXX

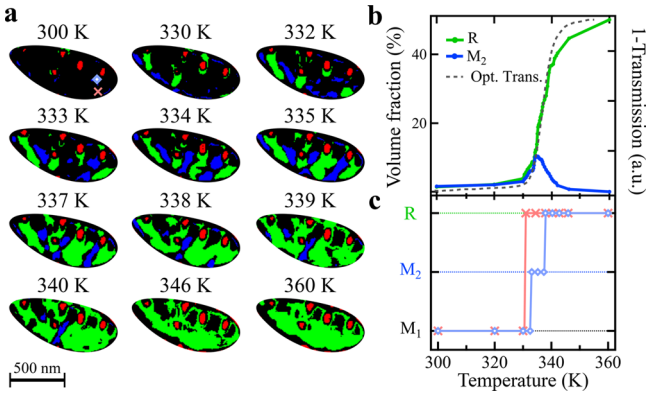

Figure 4. (a) Threshold images of domain growth in VO_2 of the single crystal outlined in Figure 3 at selected temperatures. Growth starts from defects (red) and consists of two phases, M_2 (blue) and R (green). The diamond and cross markers correspond to the ROIs used in part c. (b) Temperature-dependent growth of the two phases. The volume fraction of the M_2 phase peaks at ~335 K before the whole sample becomes metallic. The growth of the R phase is in good agreement with the change of the optical transmission measured on a witness sample. (c) Temperature dependence of the local transition pathway of the two regions marked in part a. The area marked by a red cross transitions directly from M_1 to R, while the region marked by a diamond transitions via the blue M_2 phase.

temperature, the sample is predominantly black within this color-coding scheme, indicating the presence of the initial M_1 phase, together with some defects (red). As the sample is heated, the new phases (blue, green) nucleate at the boundaries and defects of the single crystals. At intermediate temperatures (334 K), a striped state is present between regions with changes primarily in the $d_{\parallel}^{c}$ channel and in the $d_{\parallel}$ channel, before the changes tracked by the $d_{\parallel}$ feature dominate the region. This phase growth is captured in Figure 4b, which shows the volume fraction of the blue and green regions as a function of temperature within the region of interest (ROI). Both phases start to nucleate at similar temperatures and grow, before the green area dominates.

The green, $d_{\parallel}$, domains can be easily interpreted as the metallic R phase, that dominates at high temperatures. If changes in electronic correlations precede the structural transition, we would expect any green region to first turn blue as changes at $d_{\parallel}^{c}$ should occur before those at $d_{\parallel}$.[9] However, we note that most regions show a direct transition from M_1 to R without weakening of correlations. Only in some spatially distinct regions do we observe the intermediate blue regions. This is highlighted in Figure 4c, which shows the phase as a function of temperature for two nanoscale (~50 nm) regions of the sample. This indicates that the loss of correlations is not the driving mechanism for the insulator–metal phase transition as previously reported,[9] but that the two transition temperatures reported represented regions of the sample taking different pathways to the metallic phase. As strain appears responsible for nucleating the phase transition, we suggest that these blue regions can be assigned to the insulating M_2 phase, which is frequently observed in macroscopically strained samples. This assignment is further justified by recent calculations of the M_2 phase density of states, which show anisotropic changes in the d_{yz}/d_{xz} orbitals,[20] which would result in polarization-sensitive changes in the XAS in the same vicinity of $d_{\parallel}^{c}$. However, we cannot exclude that the blue regions correspond to the triclinic insulating phase, and further calculations of the XAS spectral differences for these phases are needed before a conclusive assignment can be made.

These spatially resolved measurements allow us to draw a new interpretation of the phase transition in thin films. Nanoscale defects in the thin film modify the local strain environment, locally reducing the phase-transition temperature for $M_1 \rightarrow R$. Due to the large volume difference of the R phase, a new strain field is generated which can also nucleate the M_2 phase. Both phases continue to grow and form a striped phase due to the interaction of the strain fields, as also observed in larger nanobeam single crystals.[11,12,21,22] As the temperature is further raised, a complete transformation of the M_2 to the R phase occurs. The temperature separation between the formation of M_2 and R domains for the ROI considered is approximately 5 K, in agreement with the shift in temperature observed by Gray et al.[9] This interpretation can also explain the usual temperature dependence of the XAS signal in the vicinity of $d_{\parallel}^{c}$ during a thermal cycling previously reported,[23] as the M_2 phase can be stabilized back to room temperature, although the transition temperatures and growth pattern will depend on the local distribution of strain, which will be sample specific. In our measurements, the domain patterns observed were repeatable on thermal cycling, again suggesting that strain from extrinsic defects is the dominant mechanism in these samples.[24] In the future, the role of doping impurities could potentially be examined by tuning the photon energy to be resonant to the dopant ion in order to image the homogeneity of the doping process.

In conclusion, we do not find any evidence for a new monoclinic metallic phase of VO_2, nor do we find evidence for a weakening of electronic correlations in the insulator–metal phase transition. Instead, we find that the phase transition can be explained in terms of nanoscale phase separation into the known phases of VO_2. In some respects, observation of the M_2 phase in our samples is surprising as there is no epitaxial strain provided by the substrate to move the sample away from the $M_1 \rightarrow R$ pathway. However, this work demonstrates the role nanoscale defects play in locally modifying the strain environment, which can dramatically modify the phase transition in correlated materials. Our work shows that resonant spectroholography can be used to image domain growth on the nanoscale, enabling spectroscopic measurements on samples that have a heterogeneous response. As phase separation is common in correlated materials, we believe that spectroholography will be vital in understanding the role played by defects on the structural and electronic properties in materials, such as high-temperature superconductors and colossal magnetoresistive manganites. Furthermore, when X-rays are generated by free electron lasers, holography can image domain formation and growth over a wide field of view with femtosecond time resolution, enabling imaging of the dynamics of phase transitions and coexistence during laser-driven transitions.[25]

■ ASSOCIATED CONTENT

Supporting Information

The Supporting Information is available free of charge on the ACS Publications website at DOI: 10.1021/acs.nanolett.8b00458.

Sample characterization and additional information on the performed X-ray measurements (PDF)

DOI: 10.1021/acs.nanolett.8b00458
Nano Lett. XXXX, XXX, XXX–XXX

AUTHOR INFORMATION

Corresponding Authors

*E-mail: luciana.vidas@icfo.eu.

*E-mail: simon.wall@icfo.eu.

ORCID

Simon Wall: 0000-0002-6136-0224

Notes

The authors declare no competing financial interest.

ACKNOWLEDGMENTS

L.V. and T.A.M. thankfully acknowledge financial support by the HZB. S.W. acknowledges financial support from Spanish MINECO (Severo Ochoa Grant SEV-2015-0522), Ramón y Cajal programme RYC-2013-14838, Marie Curie Career Integration Grant PCIG12-GA-2013-618487, Fundació Privada Cellex, and CERCA Programme/Generalitat de Catalunya. Research at Vanderbilt was supported by the United States National Science Foundation (EECS-1509740 for K.A.H., DMR-1207507 for R.E.M.). We thank Frank de Groot and Frederica Frati for insightful discussions.

REFERENCES

(1) Park, J. H.; Coy, J. M.; Kasirga, T. S.; Huang, C.; Fei, Z.; Hunter, S.; Cobden, D. H. Measurement of a Solid-State Triple Point at the Metal-Insulator Transition in VO_2. *Nature* **2013**, *500*, 431−434.

(2) Eyert, V. VO_2: A novel view from band theory. *Phys. Rev. Lett.* **2011**, *107*, 016401.

(3) Grau-Crespo, R.; Wang, H.; Schwingenschlögl, U. Why the Heyd-Scuseria-Ernzerhof hybrid functional description of VO_2 phases is not correct. *Phys. Rev. B: Condens. Matter Mater. Phys.* **2012**, *86*, 081101.

(4) Kim, S. H.; Kim, B. J.; Jeong, T. Y.; Lee, Y. S.; Yee, K. J. Coherent Phonon Spectroscopy of the Phase Transition in VO_2 Single Crystals and Thin Films. *J. Appl. Phys.* **2015**, *117*, 163107.

(5) Tao, Z.; Han, T.-R. T.; Mahanti, S. D.; Duxbury, P. M.; Yuan, F.; Ruan, C.-Y. Decoupling of Structural and Electronic Phase Transitions in VO_2. *Phys. Rev. Lett.* **2012**, *109*, 166406.

(6) Laverock, J.; Kittiwatanakul, S.; Zakharov, A. A.; Niu, Y. R.; Chen, B.; Wolf, S. A.; Lu, J. W.; Smith, K. E. Direct Observation of Decoupled Structural and Electronic Transitions and an Ambient Pressure Monocliniclike Metallic Phase of VO_2. *Phys. Rev. Lett.* **2014**, *113*, 216402.

(7) Liu, M. K.; Wagner, M.; Abreu, E.; Kittiwatanakul, S.; McLeod, A.; Fei, Z.; Goldflam, M.; Dai, S.; Fogler, M. M.; Lu, J.; Wolf, S. A.; Averitt, R. D.; Basov, D. N. Anisotropic Electronic State via Spontaneous Phase Separation in Strained Vanadium Dioxide Films. *Phys. Rev. Lett.* **2013**, *111*, 096602.

(8) Qazilbash, M. M.; Brehm, M.; Chae, B.-G.; Ho, P.-C.; Andreev, G. O.; Kim, B.-J.; Yun, S. J.; Balatsky, A. V.; Maple, M. B.; Keilmann, F.; Kim, H.-T.; Basov, D. N. Mott transition in VO2 revealed by infrared spectroscopy and nano-imaging. *Science* **2007**, *318*, 1750−3.

(9) Gray, A. X.; Jeong, J.; Aetukuri, N. P.; Granitzka, P.; Chen, Z.; Kukreja, R.; Higley, D.; Chase, T.; Reid, A. H.; Ohldag, H.; Marcus, M. A.; Scholl, A.; Young, A. T.; Doran, A.; Jenkins, C. A.; Shafer, P.; Arenholz, E.; Samant, M. G.; Parkin, S. S. P.; Dürr, H. A. Correlation-Driven Insulator-Metal Transition in Near-Ideal Vanadium Dioxide Films. *Phys. Rev. Lett.* **2016**, *116*, 116403.

(10) Budai, J. D.; Tselev, A.; Tischler, J. Z.; Strelcov, E.; Kolmakov, A.; Liu, W. J.; Gupta, A.; Narayan, J. In situ X-Ray Microdiffraction Studies inside Individual VO_2 Microcrystals. *Acta Mater.* **2013**, *61*, 2751−2762.

(11) Wu, J.; Gu, Q.; Guiton, B. S.; de Leon, N. P.; Ouyang, L.; Park, H. Strain-Induced Self Organization of Metal-Insulator Domains in Single-Crystalline VO_2 Nanobeams. *Nano Lett.* **2006**, *6*, 2313−2317.

(12) Liu, M.; Sternbach, A. J.; Wagner, M.; Slusar, T. V.; Kong, T.; Bud'ko, S. L.; Kittiwatanakul, S.; Qazilbash, M. M.; McLeod, A.; Fei, Z.; Abreu, E.; Zhang, J.; Goldflam, M.; Dai, S.; Ni, G.-X.; Lu, J.; Bechtel, H. A.; Martin, M. C.; Raschke, M. B.; Averitt, R. D.; Wolf, S. A.; Kim, H.-T.; Canfield, P. C.; Basov, D. N. Phase Transition in Bulk Single Crystals and Thin Films of VO_2 by Nanoscale Infrared Spectroscopy and Imaging. *Phys. Rev. B: Condens. Matter Mater. Phys.* **2015**, *91*, 245155.

(13) Tselev, A.; Lukýanchuk, I. A.; Ivanov, I. N.; Budai, J. D.; Tischler, J. Z.; Strelcov, E.; Kolmakov, A.; Kalinin, S. V. Symmetry Relationship and Strain-Induced Transitions between Insulating M1 and M2 and Metallic R phases of Vanadium Dioxide. *Nano Lett.* **2010**, *10*, 4409−4416.

(14) Eisebitt, S.; Lüning, J.; Schlotter, W. F.; Lörgen, M.; Hellwig, O.; Eberhardt, W.; Stöhr, J. Lensless Imaging of Magnetic Nanostructures by X-Ray Spectro-Holography. *Nature* **2004**, *432*, 885−888.

(15) Goodenough, J. B. The two components of the crystallographic transition in VO_2. *J. Solid State Chem.* **1971**, *3*, 490−500.

(16) Koethe, T. C.; Hu, Z.; Haverkort, M. W.; Schüßler-Langeheine, C.; Venturini, F.; Brookes, N. B.; Tjernberg, O.; Reichelt, W.; Hsieh, H. H.; Lin, H.-J.; Chen, C. T.; Tjeng, L. H. Transfer of Spectral Weight and Symmetry across the Metal-Insulator Transition in VO_2. *Phys. Rev. Lett.* **2006**, *97*, 116402.

(17) Biermann, S.; Poteryaev, A.; Liechtenstein, A. I.; Georges, A. Dynamical Singlets and Correlation-Assisted Peierls Transition in VO_2. *Phys. Rev. Lett.* **2005**, *94*, 26404.

(18) Appavoo, K.; Lei, D. Y.; Sonnefraud, Y.; Wang, B.; Pantelides, S. T.; Maier, S. A.; Jr, R. F. H. Role of Defects in the Phase Transition of VO_2 Nanoparticles Probed by Plasmon Resonance Spectroscopy. *Nano Lett.* **2012**, *12*, 780−786.

(19) Haverkort, M. W.; Hu, Z.; Tanaka, A.; Reichelt, W.; Streltsov, S. V.; Korotin, M. A.; Anisimov, V. I.; Hsieh, H. H.; Lin, H.-J.; Chen, C. T.; Khomskii, D. I.; Tjeng, L. H. Orbital-Assisted Metal-Insulator Transition in VO_2. *Phys. Rev. Lett.* **2005**, *95*, 196404.

(20) Quackenbush, N. F.; Paik, H.; Wahila, M. J.; Sallis, S.; Holtz, M. E.; Huang, X.; Ganose, A.; Morgan, B. J.; Scanlon, D. O.; Gu, Y.; Xue, F.; Chen, L.-Q.; Sterbinsky, G. E.; Schlueter, C.; Lee, T.-L.; Woicik, J. C.; Guo, J.-H.; Brock, J. D.; Muller, D. A.; Arena, D. A.; Schlom, D. G.; Piper, L. F. J. Stability of the M2 Phase pf Vanadium Dioxide induced by Coherent Epitaxial Strain. *Phys. Rev. B: Condens. Matter Mater. Phys.* **2016**, *94*, 085105.

(21) Liu, M.; Wagner, M.; Zhang, J.; McLeod, A.; Kittiwatanakul, S.; Fei, Z.; Abreu, E.; Goldflam, M.; Sternbach, A. J.; Dai, S.; West, K. G.; Lu, J.; Wolf, S. A.; Averitt, R. D.; Basov, D. N. Symmetry Breaking and Geometric Confinement in VO_2: Results from a Three-Dimensional Infrared Nano-Imaging. *Appl. Phys. Lett.* **2014**, *104*, 121905.

(22) Jones, A. C.; Berweger, S.; Wei, J.; Cobden, D.; Raschke, M. B. Nano-Optical Investigations of the Metal-Insulator Phase Behavior of Individual VO_2 Microcrystals. *Nano Lett.* **2010**, *10*, 1574−1581.

(23) Ruzmetov, D.; Senanayake, S.; Ramanathan, S. X-Ray Absorption Spectroscopy of Vanadium Dioxide Thin Films across the Phase-Transition Boundary. *Phys. Rev. B: Condens. Matter Mater. Phys.* **2007**, *75*, 195102.

(24) O'Callahan, B. T.; Jones, A. C.; Park, J. H.; Cobden, D. H.; Atkin, J. M.; Raschke, M. B. Inhomogeneity of the ultrafast insulator-to-metal transition dynamics of VO_2. *Nat. Commun.* **2015**, *6*, 6849.

(25) Dönges, S. A.; Khatib, O.; O'Callahan, B. T.; Atkin, J. M.; Park, J. H.; Cobden, D.; Raschke, M. B. Ultrafast Nanoimaging of the Photoinduced Phase Transition Dynamics in VO_2. *Nano Lett.* **2016**, *16*, 3029.

DOI: 10.1021/acs.nanolett.8b00458
Nano Lett. XXXX, XXX, XXX−XXX